Angewandte
Communications

Electrocatalysis Hot Paper

DOI: 10.1002/anie.201406112

Controlling Selectivity in the Chlorine Evolution Reaction over RuO_2-Based Catalysts**

*Kai S. Exner, Josef Anton, Timo Jacob, and Herbert Over**

***Abstract:** In the industrially important Chlor-Alkali process, the chlorine evolution reaction (CER) over a ruthenium dioxide (RuO_2) catalyst competes with the oxygen evolution reaction (OER). This selectivity issue is elucidated on the microscopic level with the single-crystalline model electrode RuO_2(110) by employing density functional theory (DFT) calculations in combination with the concept of volcano plots. We demonstrate that one monolayer of TiO_2(110) supported on RuO_2(110) enhances the selectivity towards the CER by several orders of magnitudes, while preserving the high activity for the CER. This win-win situation is attributed to the different slopes of the volcano curves for the CER and OER.*

An in-depth understanding and control of selectivity are great challenges in heterogeneous catalysis research, since the actual outcome of a branched reaction—selectivity—is governed by small energy differences in the activation energies of the competing reaction routes,[1,2] rather than by the absolute activation energies that determine the activity of a specific reaction. Although ab initio theory has developed into a powerful tool in catalysis research to gain insight into the activity of catalyzed reactions at the molecular level,[3–5] the selectivity issue is still in its infancy, particularly in electrocatalysis.

A prototypical selectivity problem in electrocatalysis is encountered with the Chlor-Alkali process, where the anodic oxidation of brine over RuO_2-based electrodes leads to the evolution of both oxygen and chlorine. From a thermodynamic point of view, the oxygen evolution reaction (OER: equilibrium potential $U^o = 1.23$ V) is preferred over the chlorine evolution reaction (CER: equilibrium potential $U^o = 1.36$ V). However, since the CER constitutes a two-electron process and the OER a four-electron process, the kinetics of the CER are much faster than that of the OER, so that the CER prevails above 1.36 V. A mixture of RuO_2 with SnO_2 or TiO_2 has been shown to improve both the stability of the electrode[6] and the selectivity of the anodic reaction towards the CER,[7] although the underlying chemistry is not well understood on a molecular level.

Over the past decade, theory[8–14] has increased our molecular understanding of electrocatalytic reactions through the use of ab initio thermodynamics.[15] Ab initio Pourbaix diagrams[9] reveal stable surface structures under (suppressed) reaction conditions, and universal scaling relationships[3] have been employed to identify the optimum adsorption properties of the electrode material for the reaction under consideration.[8,9] Here, we report the results from ab initio thermodynamics calculations on the selectivity problem of the CER and OER over RuO_2(110)-based model anodes and show how we can improve the selectivity by coating RuO_2 with a single TiO_2 layer.

A Pourbaix diagram indicates the thermodynamically most stable structure of the catalyst surface for a given electrode potential U and pH value.[16] The Pourbaix diagram relevant for both the CER and OER over RuO_2(110) takes solvation effects into account and considers the following adsorbate structures:[17] O_{br}, OH_{br}, OCl_{br}, and Cl_{br} at bridge sites as well as O_{ot}, OH_{ot}, OOH_{ot}, OCl_{ot}, Cl_{ot}, $Cl(O_{ot})_2$, $(O_{ot})_2$, and $(O_2)_{ot}$ at coordinatively unsaturated (cus) sites and all possible combinations thereof (Figure 1).

The Pourbaix diagram in Figure 2 reveals that oxygen bound on-top of Ru_{cus} atoms ($2Ru_{2f}2O_{br} + 2Ru_{cus}2O_{ot}$) is stable over a wide potential and pH range, in particular for $U > 1.36$ V, where both the CER and OER take place. At slightly higher potentials ($U > 1.49$ V) and for pH < 4, the terminal adsorption of chlorine on on-top O atoms is energetically favored so that this adsorbate structure ($2Ru_{2f}2O_{br} + 2Ru_{cus}1OCl_{ot}1O_{ot}$) can be considered as a precursor for the CER. This surface structure is consistent with the proposed reaction mechanism in the literature for the CER,[18] and therefore this transition line at 1.49 V (Figure 2) is marked with CER.

For pH > 4 and $U > 1.4$ V, another surface structure becomes energetically preferred, namely ($2Ru_{2f}2O_{br} + 2Ru_{cus}2OOH_{ot}$). This surface structure with the OOH_{ot} reaction intermediate serves as a precursor state for the OER over RuO_2(110),[8,19] while the CER cannot occur on this surface structure. Therefore, the transition from the fully O-covered RuO_2(110) surface to ($2Ru_{2f}2O_{br} + 2Ru_{cus}2OOH_{ot}$) is indicative of the OER (Figure 2).

From recent theoretical studies,[8,9,19] the reaction mechanisms of the CER and the OER over RuO_2(110) are considered to be settled. The CER proceeds through the so-

---

[*] K. S. Exner, H. Over
Physical Chemistry Department, Justus-Liebig-University Giessen
Heinrich-Buff-Ring 58, 35392 Giessen (Germany)
E-mail: Herbert.Over@phys.Chemie.uni-giessen.de

J. Anton, T. Jacob
Institute of Electrochemistry, Ulm University
Albert-Einstein-Allee 47, 89069 Ulm (Germany)

[**] K.S.E. acknowledges financial support by the Fonds der Chemischen Industrie (FCI) through a PhD scholarship. H.O. was supported by the LOEWE program STORE_E within the Laboratory of Materials Research at the JLU. T.J. acknowledges support from the European Research Council through the ERC-Starting Grant THEOFUN (Grant Agreement No. 259608). We thank the DFG (Deutsche Forschungsgemeinschaft) for financial support through the priority program (SPP1613).

Supporting information for this article is available on the WWW under http://dx.doi.org/10.1002/anie.201406112.

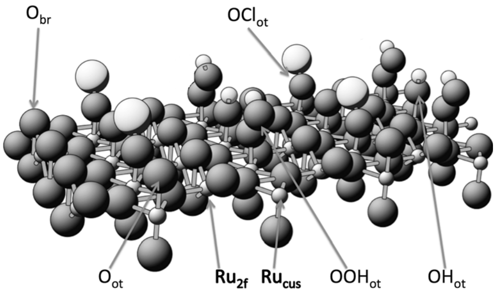

Figure 1. Various adsorbates on the $RuO_2(110)$ surface are shown which are relevant as reaction intermediates in the CER and OER. The metal atoms are indicated as small balls, while oxygen (dark gray) and chlorine (light gray) are shown as larger balls. Hydrogen atoms are displayed as small light gray balls. The surface of bare $RuO_2(110)$ exposes coordinatively under-coordinated Ru sites (Ru_{cus}) and under-coordinated oxygen sites (O_{br}) which bridge two Ru_{2f} sites underneath. Adsorbates bridging two Ru_{2f} atoms are denoted with the index "br" and adsorbates in terminal position on Ru_{cus} atoms with the index "ot" (on-top). For example, O_{ot} are on-top oxygen atoms which are attached to Ru_{cus} sites. The nomenclature of the surface structure is referred to a (2×1) unit cell, indicating all the surface species in the unit cell including the attached metal atoms. For example, $(2Ru_{2f}2O_{br}+2Ru_{cus}2O_{ot})$ contains two O_{br} bridging two Ru_{2f} sites, and two on-top oxygen atoms O_{ot} attached to Ru_{cus} sites.

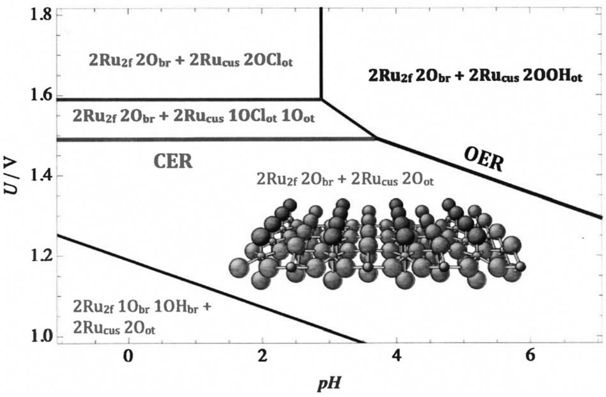

Figure 2. Pourbaix diagram for the model catalyst $RuO_2(110)$ in equilibrium with H^+, Cl^-, and H_2O at $T=298$ K and $a(Cl^-)=1$. The adsorbate structure $2Ru_{2f}2O_{br}+2Ru_{cus}2O_{ot}$ constitutes the thermodynamically most stable surface under reaction conditions for the CER (thick gray) and for the OER (thick black).[17] Mechanistically, the OCl_{ot} adsorbate constitutes the precursor for the CER, whereas the OOH_{ot} adsorbate serves as the molecular precursor for the OER.

called Volmer–Heyrovsky mechanism,[18,20] where the adsorption and discharge of a chloride ion [Eq. (1)]

$$2O_{ot} + Cl^- \rightarrow O_{ot} + OCl_{ot} + e^- \text{ (Volmer step)} \tag{1}$$

is followed by the direct recombination of this adsorbed chlorine species with a chloride ion from the electrolyte solution accompanied by an electron transfer and the release of Cl_2 [Eq. (2)]:

$$O_{ot} + OCl_{ot} + Cl^- \rightarrow 2O_{ot} + Cl_2 + e^- \text{ (Heyrovsky step)} \tag{2}$$

Altogether, the CER constitutes a two-electron process.

The OER constitutes a four-electron process. Assuming a coupled electron–proton transfer,[8] the reaction mechanism can be formulated as shown in Equations (3)–(6).

$$2O_{ot} + H_2O \rightarrow 1O_{ot}1OOH_{ot} + H^+ + e^- \tag{3}$$

$$1O_{ot}1OOH_{ot} \rightarrow 1O_{ot} + O_2 + H^+ + e^- \tag{4}$$

$$1O_{ot} + H_2O \rightarrow 1O_{ot}1OH_{ot} + H^+ + e^- \tag{5}$$

$$1O_{ot}1OH_{ot} \rightarrow 2O_{ot} + H^+ + e^- \tag{6}$$

In general, the change in the Gibbs energy for a one-electron process is given by $\Delta G=\Delta G^0-e\,U^o$, where U^o is the equilibrium potential for the CER or the OER. The changes in the Gibbs energy ΔG_j^0 for each electron transfer step j are accessible by DFT calculations (see the Supporting Information) at the electric potential $U=0$ V. The step with the most unfavorable Gibbs energy change at the equilibrium potential defines the loss in the Gibbs energy ΔG_{loss}.[12] ΔG_{loss} represents the thermodynamic barrier in the overall process and, therefore, the activity. Figure 3a depicts the variations in the Gibbs

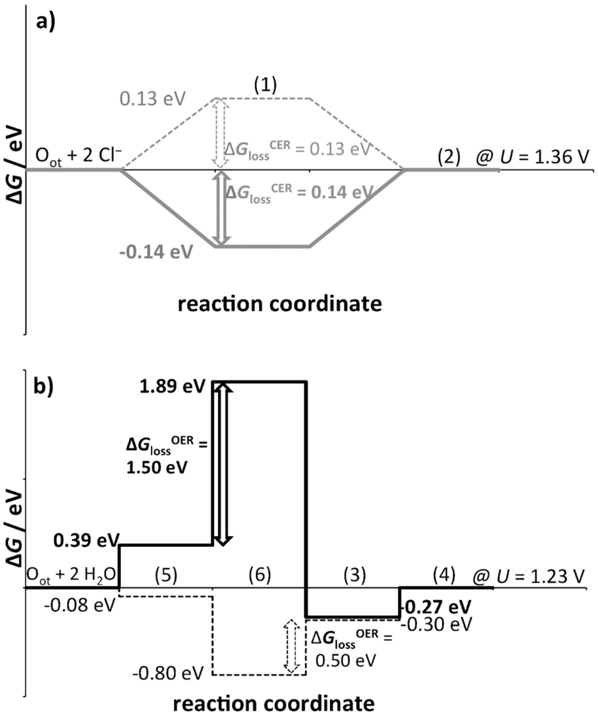

Figure 3. Gibbs energy diagram for the a) CER (gray) and for the b) OER (black) over the fully O-covered $RuO_2(110)$ surface (dashed line) and for the Ti-substituted fully O-covered $RuO_2(110)$ surface (solid line). a) For the CER over the fully O-covered $RuO_2(110)$ surface, the step with the most unfavorable Gibbs energy change ($\Delta G_{loss}{}^{CER}$) constitutes the adsorption of chlorine, whereas for the Ti-modified $RuO_2(110)$ surface, the formation of gaseous chlorine defines the Gibbs energy loss. b) For the OER over the fully O-covered $RuO_2(110)$ surface, the step with highest Gibbs energy change constitutes the splitting of the second water molecule accompanied by the formation of the OOH_{ot} adsorbate structure, whereas for the Ti-modified $RuO_2(110)$ surface the formation of the O_{ot} adsorbate suffers from the highest change in Gibbs energy ($\Delta G_{loss}{}^{OER}$). The reference states for CER and OER over $RuO_2(110)$ are identical, while these are different on Ti-modified $RuO_2(110)$.

energy for the CER over $RuO_2(110)$-based anodes according to reaction steps (1) and (2) and an equilibrium potential $U^{o} = 1.36$ V. In the case of $RuO_2(110)$, the adsorption of Cl^- is the most energy-demanding step in the CER by $\Delta G_{loss}{}^{CER} = 0.13$ eV (broken line in Figure 3a). The variations in the Gibbs energy are shown in Figure 3b for the OER over RuO_2-based electrocatalysts (reaction steps (3)–(6)) and an equilibrium potential $U^{o} = 1.23$ V. In the case of $RuO_2(110)$, the formation of OOH_{ot} is the most energy-demanding step, which results in $\Delta G_{loss}{}^{OER} = 0.50$ eV (broken line in Figure 3b). Both values of ΔG_{loss} can also be represented in the Pourbaix diagram (see Figure S2 in the Supporting Information).

The thermodynamic barriers for the CER and OER over $RuO_2(110)$ are not zero, so there is still room for improvement. How should we modify the electrode to decrease the ΔG_{loss} values for the CER and OER? Based on the Sabatier principle, the adsorption energy of oxygen provides a universal descriptor for the reactivity of metal oxide surfaces in oxidation catalysis.[3,21–23] Hansen et al.[9] confirmed for the CER and Rossmeisl et al.[8] confirmed for the OER that the free adsorption energy of oxygen is indeed an appropriate descriptor for these anodic oxidation reactions. Therefore, the activity of the CER or OER in terms of the loss of Gibbs energy establishes so-called volcano plots as a function of the free oxygen adsorption energy (Figure 4).

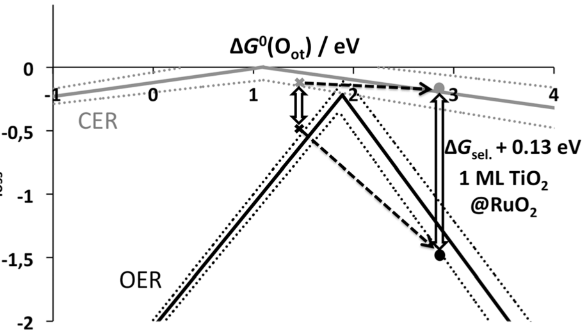

Figure 4. Volcano plot for the CER (gray) and for the OER (black) over $RuO_2(110)$. The size of the lines (indicated by the dotted lines) reflects the standard deviations as a result of the standard deviations in the linear scaling relations. The gray cross denotes the catalytic activity (ΔG_{loss}) of the $RuO_2(110)$ catalyst for the CER and the black cross that for the OER. The difference in Gibbs energy losses defines the selectivity, as quantified by ΔG_{sel}. For the case of $RuO_2(110)$, ΔG_{sel} amounts to 0.24 eV. Weakening the ruthenium–oxygen bond will marginally affect the catalytic activity for the CER. However, weakening the ruthenium–oxygen bond leads to a much lower catalytic activity in the OER, thus improving the selectivity substantially. The reduction of the O_{ot} free adsorption energy from 1.43 eV to 2.88 eV can be realized by 1ML of $TiO_2(110)$ on $RuO_2(110)$ (solid points). The resulting selectivity is quantified by $\Delta G_{sel} = 1.23$ eV.

To construct a volcano plot, the linear scaling relations between the free adsorption energies of OCl_{ot} (for the CER) and OH_{ot}, OOH_{ot} (for the OER) as a function of the free adsorption energy of O_{ot} to the catalyst's surface $\Delta G^0(O_{ot})$ need to be evaluated (computational details on the construction of the volcano plots can be found in the Supporting Information).

Volcano plots arise when two competing processes determine the activity. In the case of the CER, high values of $\Delta G^0(O_{ot})$ (weak O_{ot} adsorption; right leg) lead to Cl^- desorption being limiting, while small values of $\Delta G^0(O_{ot})$ (left leg) lead to the Cl^- adsorption becoming limiting. In the case of the OER, high values of $\Delta G^0(O_{ot})$ (right leg) impede OOH_{ot} decomposition, while for small values of $\Delta G^0(O_{ot})$ (left leg) the formation of OH_{ot} is hampered. In between, the CER and OER proceed with maximum activity.

The volcano plot for the CER is quite flat compared to that of the OER. This difference in the slopes reflects the number of reaction intermediates in the CER and OER: one versus three. For the CER, the volcano plot indicates the loss in Gibbs energy is (0.1 ± 0.1) eV in the $\Delta G^0(O_{ot})$ range of 0.3 eV to 2.2 eV, while for the OER the minimum value of $\Delta G_{loss}{}^{OER}$ is 0.22 eV at $\Delta G^0(O_{ot}) = (1.89 \pm 0.05)$ eV. This minimum value of $\Delta G_{loss}{}^{OER}$ has also been found by Rossmeisl et al.[8] and was rationalized by the requirement to stabilize various reaction intermediates whose adsorption energy cannot be optimized with a single descriptor $\Delta G^0(O_{ot})$. For the fully O-covered $RuO_2(110)$ surface ($2Ru_{2f}2O_{br} + 2Ru_{cus}2O_{ot}$), the actual Gibbs energy losses of 0.13 eV and 0.5 eV for the CER and OER, respectively, are indicated as crosses in Figure 4.

The selectivity for the CER is determined by the difference in the Gibbs free energy ΔG_{sel} between $\Delta G_{loss}{}^{CER}$ and $\Delta G_{loss}{}^{OER}$ when both losses are referenced to the same potential $U^{o} = 1.36$ V and additional kinetic barriers are ignored; note that $\Delta G_{loss}{}^{OER}$ is originally referred to 1.23 V and must be reduced accordingly by 1.36–1.23 eV = 0.13 eV. For the case of $RuO_2(110)$, ΔG_{sel} amounts to 0.24 eV. This quantity can also be included in the Pourbaix diagram (see Figure S2 in the Supporting Information) as an additional feature. For $\Delta G_{sel} = 0.24$ eV in favor of the CER, a branching ratio between the CER and OER of about 10^4 is derived at $T = 298$ K, which is compatible with experimental values.[7]

By inspecting the volcano curves in Figure 4, a straightforward strategy to improve the selectivity without deteriorating the activity of the CER is to reduce the O_{ot} free adsorption energy by 1.5 eV. With this shift in the free O_{ot} adsorption energy, the activity of the CER is preserved, while the $\Delta G_{loss}{}^{OER}$ increases substantially by about 1 eV as we follow the other arm downwards in the OER volcano. This win-win situation is due to different slopes of the volcano curves of the CER and OER.

In fact, this favorable situation can even be realized by replacing the topmost Ru atoms by Ti so that the O_{ot} free adsorption energy is weakened by about 1.5 eV. The computed ΔG_{loss} values for this Ti-modified $RuO_2(110)$ electrode surface are indicated as solid points in the volcano plot (Figure 4).

The Gibbs energy diagrams of the CER and OER over the Ti-substituted $RuO_2(110)$ surface are shown in Figure 3 (solid lines). Here we can recognize that not only the Gibbs energy loss but also the reaction control has changed when the topmost Ru layer $RuO_2(110)$ surface is substituted by Ti. For the CER, the adsorption of Cl^- defines the reaction step with the highest Gibbs energy change for $RuO_2(110)$, while the recombination of adsorbed Cl with a Cl^- ion from the solution is mostly uphill in free energy for the Ti-substituted $RuO_2(110)$. For the OER, the formation of OOH_{ot} is the step with the highest Gibbs change for $RuO_2(110)$, but for the case of Ti-substituted $RuO_2(110)$, the formation of O_{ot} defines the step with the Gibbs energy loss.

Only a single layer of $TiO_2(110)$ on $RuO_2(110)$ leads to excellent selectivity and good activity for the CER. According to our calculations, a double or a triple layer of $TiO_2(110)$ on $RuO_2(110)$ degrades the activity for the CER substantially, as expressed by the determined Gibbs energy losses of 0.35 eV and 1.08 eV, respectively. The reason for this behavior lies in the too weak bonding of O_{ot} so that the terminal chlorine adsorption becomes too strong, accompanied by the large Gibbs energy losses in the Heyrovsky step. When reducing the coverage of TiO_2 below one monolayer (1 ML), for example by substituting only the cus-Ru atoms by Ti, then the activity in the CER is slightly improved with reference to $RuO_2(110)$ ($\Delta G_{loss} = 0.10$ eV), but the selectivity is substantially lower than for the 1 ML TiO_2 case, as quantified by $\Delta G_{sel} = 0.91$ eV.

In heterogeneous catalysis, TiO_2 is frequently used as a carrier, supporting the active component in the form of metal or oxide clusters. The 1ML TiO_2/RuO_2 system may therefore be envisioned as a positive example of strong metal–support interactions in catalysis.[24–26] A single layer of $TiO_2(110)$ grown on $RuO_2(110)$ increases the selectivity between the chlorine and oxygen evolution reactions by several orders of magnitude, while keeping the high activity for the CER virtually constant.

Received: June 11, 2014

Keywords: chlorine evolution · density functional calculations · electrocatalysis · ruthenium dioxide · selectivity

---

[1] G. Ertl, H. Knözinger, F. Schüth, J. Weitkamp, *Handbook of Heterogeneous Catalysis*, VCH, Weinheim, **2008**.
[2] J. M. Thomas, W. J. Thomas, *Principles and Practice of Heterogeneous Catalysis*, VCH, Weinheim, **1997**.
[3] J. K. Nørskov, T. Bligaard, J. Rossmeisl, C. H. Christensen, *Nat. Chem.* **2009**, *1*, 37.
[4] M. Neurock, *Ind. Eng. Chem. Res.* **2010**, *49*, 10183.
[5] R. A. Van Santen, M. Neurock, S. G. Shetty, *Chem. Rev.* **2010**, *110*, 2005.
[6] a) S. Trasatti, *Electrochim. Acta* **2000**, *45*, 2377; b) A. R. Zeradjanin, T. Schilling, S. Seisel, M. Bron, W. Schuhamnn, *Anal. Chem.* **2011**, *83*, 7645.
[7] T. Arikawa, Y. Murakami, Y. Takasu, *J. Appl. Electrochem.* **1998**, *28*, 511.
[8] J. Rossmeisl, Z.-W. Qu, H. Zhu, G.-J. Kroes, J. K. Norskov, *J. Electroanal. Chem.* **2007**, *607*, 83.
[9] H. A. Hansen, I. C. Man, F. Studt, F. Abild-Pedersen, T. Bligaard, J. Rossmeisl, *Phys. Chem. Chem. Phys.* **2010**, *12*, 283.
[10] J. A. Keith, G. Jerkiewicz, T. Jacob, *ChemPhysChem* **2010**, *11*, 2779.
[11] C. D. Taylor, S. A. Wasileski, J. S. Filhol, M. Neurock, *Phys. Rev. B* **2006**, *73*, 165402.
[12] A. B. Anderson, *Electrocatalysis* **2012**, *3*, 176.
[13] F. Calle-Vallejo, M. T. M. Koper, *Electrochim. Acta* **2012**, *84*, 3.
[14] M. T. M. Koper, *Chem. Sci.* **2013**, *4*, 2710.
[15] T. Jacob in *Fuel Cell Catalysis: A Surface Science Approach* (Eds.: M. T. M. Koper, A. Wieckowski), Wiley, Hoboken, **2009**, pp. 129–158.
[16] *Atlas of Electrochemical Equilibria in Aqueous Solutions* (Ed.: M. Pourbaix), NACE, Houston, TX, **1974**.
[17] K. S. Exner, J. Anton, T. Jacob, H. Over, *Electrochim. Acta* **2014**, *120*, 460.
[18] V. Consonni, S. Trasatti, F. Pollak, W. E. O'Grady, *J. Electroanal. Chem.* **1987**, *228*, 393.
[19] Y.-H. Fang, Z.-P. Liu, *J. Am. Chem. Soc.* **2010**, *132*, 18214.
[20] L. J. J. Janssen, L. M. C. Starmans, J. G. Visser, E. Barendrecht, *Electrochim. Acta* **1977**, *22*, 1093.
[21] Y. D. Pankratiev, *React. Kinet. Catal. Lett.* **1982**, *20*, 255.
[22] S. Trasatti, W. E. O'Grady in *Advances in Electrochemistry and Electrochemical Engineering*, *Vol. 13* (Eds.: H. Gericher, C. W. Tobas), Wiley, New York, **1980**, p. 177.
[23] S. Trasatti, *Electrochim. Acta* **1984**, *29*, 1503.
[24] S. J. Tauster, S. C. Fung, R. T. K. Baker, J. A. Horsley, *Science* **1981**, *211*, 1121.
[25] T. Uchijima, *Catal. Today* **1996**, *28*, 105.
[26] Q. Fu, T. Wagner, *Surf. Sci. Rep.* **2007**, *62*, 431.